ROMANIAN JOURNAL OF INFORMATION SCIENCE AND TECHNOLOGY
Volume **13**, Number 1, 2010, 3–21

Nickel MEMS Energy Harvesters for the Self-Powering of Vehicular Sensing Systems

Giorgio DE PASQUALE[1], Mian WEI[2]

[1] Mechanical Department, Politecnico di Torino,
Corso Duca degli Abruzzi 24, 10129, Torino, Italy
E-mail: giorgio.depasquale@polito.it

[2] Electrical Engineering Department, University of South Florida,
4202 East Fowler Avenue, 33620, Tampa, USA
E-mail: mwei@mail.usf.edu

Abstract. MEMS energy harvesters are attracting researchers' attentions from both academia and industries for the self-powering of sensing systems in vehicular applications. The possibility to convert the power contained in the mechanical vibrations into electrical power offers the possibility to replace traditional wired sensors with wireless devices, to simplify the on-board architecture, increase maintainability and reduce operative and supplying costs. This work describes the design and fabrication of vibrating harvesters using electroplated nickel as the structural material; a modular approach is proposed for the mask definition of compact self-powered sensing systems. The capacitive transduction principle is adopted for ease of fabrication and efficient conversion. In addition, some strategies to improve the dynamic performances in terms of resonance frequency tuning and bandwidth amplification are also presented.

1. Introduction

Small and large vehicles (automotive, railway, aircrafts, etc.) need to be aided during their work by several sensors and other small devices in order to monitor the proper functioning of all sub-systems and components and to provide the instantaneous measurement of the most relevant environmental parameters [1, 2]. On-board sensors, or sensors networks, are usually supplied by the electric power generated by the engine of the vehicle and transferred from the main battery to the small detector by means of wires. The needing to monitor a large amount of parameters (e.g. for

aerospace vehicles) causes the proliferation of electrical wires, leading to very complicated sensing architectures and many other problems related to the maintenance and reliability. The amount of electrical power required by the on-board sensing system also causes additional fuel consumption and the consequent pollution.

A new approach was recently investigated for the supply of on-board sensing systems, which is based on the self-powering by means of micro power generators. This idea starts from the evidence that a large amount of mechanical vibrations characterizes all vehicles and mass transportation systems during their operations [3]. The conversion of the mechanical power associated to vibrations into electrical power is commonly identified as the key-solution for the self powering of on-board sensing systems. Open problems and future challenges of this field are related to the design and fabrication of the devices able to convert the power with reasonable efficiency and reliability, with low cost building processes and large scales applicability. The micro electro-mechanical systems (MEMS) technology seems to be the most suitable one to satisfy the above mentioned requirements and to allow the fabrication of energy harvesters [4]. MEMS technology allows the fabrication of microsystems that are able to harvest energy from the environment to power sensors in small scale for vehicles applications and a variety of other fields such as structural health monitoring, process control and health care. Despite several power sources readily available from ambient can be ideally utilized to generate power (including solar energy [5], temperature gradients, fluidic flows, and pressure variations), mechanical vibrations are definitely the most attractive for vehicular applications from an energetic balance viewpoint. Different mechanisms were investigated in the literature to convert the power by using MEMS devices; three strategies were identified and adopted in previous works to design energy harvesters: capacitive, piezoelectric and magnetic-inductive [6–8]. Each of them is characterized by specific advantages and limitations. A complete review about present theories and applications is represented by [9, 10].

Vehicular sensing monitoring is usually related to motion and environmental parameters detection, passengers comfort improvement, components damage control and prevention. The architecture of traditional sensing networks adopted in this field has a low versatility due to the usage of wired electrical connections and battery power. The same limitations are present in operative applications and laboratory setup configurations. Networks based on locally supplied sensors need not electrical connections to be powered; besides a wireless transmission can be used to send the measured parameters to the central unit acting as data postprocessor. Several design challenges are related to the development of MEMS energy harvesters, such as the dynamic dimensioning, the power efficiency and the structural reliability. The optimal energy harvesting efficiency is obtained when the device is operating under resonance conditions, thus demanding design methodologies to fine-tune the resonance frequency to match with that of the infrastructures under surveillance. A wider bandwidth is thus preferred to accommodate any variation in the dynamic excitation induced by the ambient vibration.

This work reports the activity of design and fabrication of MEMS-based energy harvesters for scavenging vibration energy in the range of 300–700 Hz. The capacitive transduction was adopted mainly for the following two reasons: the fabrication process

required is less complicated and expensive than that of piezoelectric devices and the expected reliability is better than that of their magnetic counterparts. Static and modal FEM simulations were conducted for optimizing the dynamic response of the design. The nickel electroplating process was employed for low-cost fabrication and modular integration with ICs.

2. Design issues

Design of sensing platform architecture representing each node of the wireless sensor network is based on the preliminary analysis of functional parameters of the device, such as energetic balance, range of working frequencies, volume and operative conditions imposed by the final application. The design variables above indicated are applicable on a basic configuration; this configuration includes one or more harvesters, a storage battery for power accumulation, one or more sensors, and a wireless RF transceiver. Electrical conditioning and components integration are very important to assure a proper functionality. Some examples of suitable strategies at this purpose are reported in [11–13]. Maximization of the device efficiency in terms of the energy conversion needs the optimization of the material properties, of the manufacturing processes and of the properties of the electrical components [14]. Figures of merit in terms of density of power scavenged per unit of volume demonstrate that conversion from mechanical vibration into electrical charge and voltage looks effective and suitable to be applied in many industrial micro applications [3, 15].

Numerical simulation strategies, compact analytical models and experimental validation on dedicated specimens are exploited to perform predictive analyses of static and dynamic behavior of microstructures. Structural properties of moving parts need static and dynamic analyses in order to define fundamental design parameters for their operation. In practice, the performance of these systems is measured in terms of power scavenged per unit of volume/area and operating frequency bandwidth. Power harvested depends on the geometry of the scavenger and on the layout of the electric circuit connected, including the energy storage system. Frequency bandwidth strongly depends on the inertial and stiffness properties of the microstructure deserving as scavenger.

In case of capacitive harvesters, the static relation between voltage and displacement is directly related to the pull-in voltage of the device. Electromechanical coupling is directly responsible of typical effects such as the resonance frequency shift and the structural stiffening/softening in the frequency domain, caused by the nonlinearity of the coupling. The presence of residual stress/strain after fabrication process, studied in [16], requires the formulation of dedicated modeling strategies. A preliminary design activity concerns the kinematics of movable structures. There are mainly three suitable strategies (Fig. 1): in-plane gap closing, in-plane overlap and out-of-plane. Each of them is dominated by the effects of nonlinearity of the electromechanical coupling. Several examples of nonlinearities associated to the design of microstructures are reported in [17, 18]. The presence of air surrounding the movable structures is a source of dissipative and elastic phenomena described by microfluidic relations that

are strongly dependant on the geometry of components, frequency and outer pressure; numerical and compact analytical approaches have been defined for the modeling in [19, 20]. An important issue for the reliability prediction is the analysis of the fatigue behavior of microstructures in presence of alternate cyclic loads [21–23]. Modeling strategies already consolidated for macromechanical applications are nowadays applied to the experiments at microscale. Dedicated test structures were built and experimental settings were defined: fundamental methods for specimens design and several experimental tests are described respectively in [24] and [25].

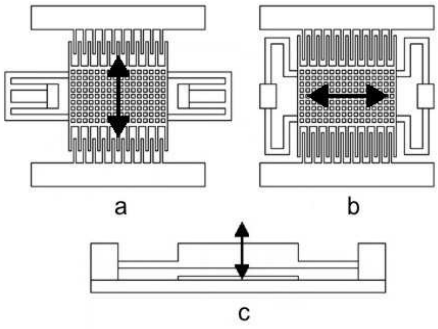

Fig. 1. Sketch of three common design strategy for capacitive harvesters: in-plane overlap (a), in-plane gap closing (b) and out-of-plane (c).

Tuning the resonance of the vibration energy harvester on the frequency of the external excitation is a key feature of the design [26]. The development of strategies for the tuning of scavenger resonance frequency is fundamental to increase the global efficiency of the device for applications characterized by wide frequency spectra; for instance, in [27] a resonance tuning technique of a piezoelectric scavenger is described. This task is required to get the maximum power available for the conversion. Nevertheless, a precise cognition of the frequency of the exciting vibration is very seldom possible. This problem is usually overcome by adding a frequency tuning strategy to the scavenger, to match the maximum vibration power at the actual frequency of the excitation. A first possibility is building up a set of harvesters with different geometry, i.e. microbeams of different length [28], all tuned on a precise value of resonance frequency, within the required bandwidth. If only a single device is preferred, an inertial damper equivalent system can be designed [29]. In practice, if an auxiliary and smaller structure is suitably connected to the main frame, by a compliant elastic joint, whose stiffness is known, the frequency spectrum shows two main resonances very close to the eigenmode of the main frame. This makes wider the bandwidth at which the energy harvesting is effective [30]. Other strategies observe that stiffness is more controllable than inertia, therefore a regulation can be performed by stiffening or softening the resonant microstructure [31]. Tuning techniques currently tested and proposed in the literature concern mainly piezoelectric devices, although some strategies apply to the electrostatic scavenger too. In particular, when energy conversion is played by means of the structural bending of a flexible microbeam or microplate,

if an axial load is applied, resonance of the selected eigenmode changes, thanks to the axial-flexural coupling and is lowered as far as is stronger the compressive action applied [29, 31]. The lowering of resonance frequency of MEMS structures is another important design issue for applications in the dynamic range of vehicles. The proper choose of the vibrating proof mass and the correct modeling of the structural stiffness are important to obtain a low resonance; meander springs are usually adopted to reduce the global stiffness. An example of magnetic suspensions for MEMS harvesters was proposed in [32] in order to avoid physical connections between the proof mass and the ground and to minimize the global stiffness. All the above mentioned aspects will be investigated in this paper, being aimed at studying the electromechanical conversion of mechanical vibrations into electric power by means of MEMS technology [33, 34].

3. Geometry and electro-mechanical properties

The capacitive energy harvesting is based on generation of current by the relative displacement between two charged electrodes. The movable electrode is usually connected to a proof mass suspended on elastic springs. Several kinematic approaches can be adopted to provide the relative displacement between electrodes (Fig. 1). The in-plane solution with comb drives however allows maximizing the output power compared to the out-of-plane strategy. Capacitors operate in constant voltage when the proof mass moves along the plane of the comb (Fig. 1a), while they operate in constant charge when the mass moves perpendicularly to the combs (Fig. 1b). In practice, in case of a simple industrial implementation, basic parameters to be dimensioned are average gap, area, thickness and structural stiffness of suspensions [34]. Stiffness of suspensions and plate mass must be designed properly to tune the MEMS resonance on the excitation frequency range. Electrostatic converters are benefited by the presence of stop dimples used to avoid pull-in instability.

3.1. Geometrical design

Two different designs are proposed (design A and B). In the first one the capacitance change is produced by a variation of the overlap area between electrodes (overlap strategy), in the second case by a variation of the gap between the electrodes (gap closing strategy). The overlap solution provides a linear relation between the mass displacement and the output voltage (instead this relation is nonlinear in the gap closing solution). The output voltages between the electrodes on the two sides of the center proof-mass are in-phase for the gap closing scenario, while there is a 180° phase shift for the case of varying overlap. A large central proof mass and two side comb-shaped electrodes were provided for both designs. Several variants in geometrical dimensions were introduced in the designs to determine the dynamic and electrical responses. The definition of mass (m) and static stiffness (k_{st}) of springs is responsible for the natural frequency of the device. The geometrical characteristics of comb drives are responsible for controlling the electrical power output. Figure 2

presents the schematics of designs A and B in which the key dimensions are specified. The maximum oscillation amplitude is limited by the presence of stop dimples (indicated by o).The exact dimensions for all variants of the two designs are reported in Tab. 1.

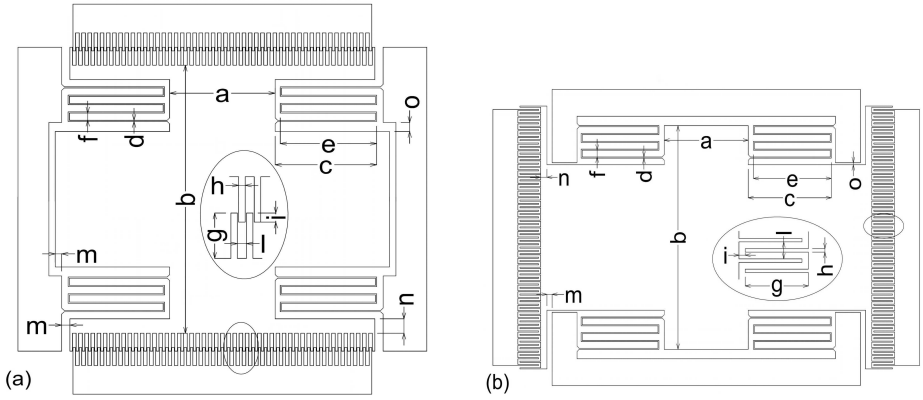

Fig. 2. Schematics of designs A (a) and B (b).

The device thickness is $t = 100$ μm; the static stiffness was calculated by a FEM model as the ratio between a static force and the resultant displacement of the suspended proof-mass. The modal mass (m_{mod}) is that portion of the total mass which participates to the first modal shape. The second modal frequency was determined, which must be sufficiently higher to avoid the coupling effect between adjacent modal shapes and the related misalignments among comb drives. The first and the second resonance frequencies, static stiffness, total and modal mass are reported in Tab. 1 for each variant.

The efficient deployment of energy harvesters in vehicular applications demands the resonance frequency of the device to reside at relatively low frequencies on the order few hundreds of Hertz. This requires the integration of a huge proof mass and low stiffness. By using the same symbols of Tab. 1, some properties of harvesters can be defined for design A as: the number of capacitors $N_A = 4(a+2c-h)/(l+h)$, the maximum area $A_{\max} = t(i+o)$ and the minimum area $A_{\min} = ti$ of each variable capacitor and the gap between the parallel-plate capacitor $x=(l-h)/2$. For design B the number of capacitors $N_B=4[(a+2c-h)/(l+h)–1]$, the maximum gap $x_{\max}=(l-h)/2+o$ and the minimum gap $x_{\min}=(l-h)/2–o$ between two capacitor electrodes and the overlap area of capacitor $A = t(g–2i)$.

3.2. Bandwidth amplification

A large bandwidth is required for energy harvesters in order to maximize the oscillation amplitude of the proof mass within a specific frequency range. This characteristic is needed because the frequency of vibration generated by the vehicle is no longer constant in real applications but may vary around a nominal value. Several strategies can be adopted to amplify the bandwidth of vibrating devices. First possibility is to build a set of harvesters with different geometry [28] all tuned on a precise

value of resonance frequency. Other strategies provide the desired resonance tuning by stiffening/softening the suspension structure by means of axial loads [31], or the application of electrical preloads to vary the global stiffness [26].

Tab. 1. Geometrical dimensions and structural properties for all variants of designs A and B

Design	Geometrical dimensions [μm]													Resonance freq. [Hz]		k_{st}	m	m_{mod}
	a	b	c	d	e	f	g	h	i	l	m	n	o	Mode I	Mode II	[μN/μm]	[10^{-5}kg]	[10^{-5}kg]
A1	810	2000	800	10	750	75	100	10	10	14	50	60	75	484	879	30.1	0.33500	0.33014
A2	802						100	10	10	16		60		486	886		0.33215	0.32729
A3	802						150	10	60	16		60		480	860		0.34043	0.33557
A4	820						100	20	10	28		120		484	811		0.33482	0.32996
A5	820						150	20	60	28		120		478	787		0.34390	0.33904
A6	610		900		850		100	10	10	14		60		417	813	21.2	0.31898	0.31354
A7	602						100	10	10	16		60		419	820		0.31613	0.31069
A8	602						150	10	60	16		60		414	795		0.32441	0.31897
A9	620						100	20	10	28		120		417	743		0.31880	0.31336
A10	620						150	20	60	28		120		411	720		0.32788	0.32244
A11	410		1000		950		100	10	10	14		60		367	765	15.4	0.30296	0.29694
A12	402						100	10	10	16		60		369	772		0.30011	0.29410
A13	402						150	10	60	16		60		363	747		0.30839	0.30237
A14	420						100	20	10	28		120		367	693		0.30278	0.29676
A15	420						150	20	60	28		120		361	671		0.31186	0.30584

Design	Geometrical dimensions [μm]													Resonance freq. [Hz]		k_{st}	m	m_{mod}
	a	b	c	d	e	f	g	h	i	l	m	n	o	Mode I	Mode II	[μN/μm]	[10^{-5}kg]	[10^{-5}kg]
B1	810	2000	800	10	750	60	100	10	10	30	50	60	8	419	848	31.2	0.45913	0.45434
B2							150		10	30			8	417	832		0.46456	0.45977
B3							200		10	30			8	414	817		0.46999	0.46520
B4							100		10	50			18	421	858		0.45557	0.45078
B5							200		20	50			18	418	836		0.46287	0.45808
B6							300		20	50			18	414	813		0.47017	0.46538
B7	610		900		850		100		10	30			8	356	790	21.9	0.44845	0.44307
B8							150		10	30			8	354	775		0.45388	0.44850
B9							200		10	30			8	351	760		0.45931	0.45393
B10							100		10	50			18	357	800		0.44489	0.43951
B11							200		20	50			18	354	779		0.45219	0.44681
B12							300		20	50			18	351	757		0.45949	0.45411
B13	410		1000		950		100		10	30			8	308	745	15.9	0.43777	0.43181
B14							150		10	30			8	306	730		0.44320	0.43724
B15							200		10	30			8	304	716		0.44863	0.44267
B16							100		10	50			18	309	754		0.43421	0.42825
B17							200		20	50			18	306	734		0.44151	0.43555
B18							300		20	50			18	304	713		0.44881	0.44285

The solution adopted here is to couple several identical energy harvesting devices with the same dimensions and shape to form a mechanically-coupled composite device with intermediate springs with variable stiffness. The resulting frequency response function (FRF) of the coupled harvester is characterized by a number of resonance peaks corresponding to the number of proof masses connected. The resultant resonances and the bandwidth are dependent to the stiffness of intermediate springs. The advantages of this approach are the design simplification (the same shape and dimensions are used for all the harvesters), and the possibility to obtain variable bandwidth

amplitudes using different springs. The spring characteristic can be changed also by means of the stiffening/softening strategy by using additional components able to provide static axial loads. Three different spring types were designed and built, as reported in Fig. 3. Their stiffness values from FEM simulation are $k_1 = 23.2$ μN/μm, $k_2 = 11.0$ μN/μm and $k_3 = 7.2$ μN/μm for types 1, 2 and 3 respectively. The gap closing harvesters identified by designs B1, B7 and B13 were used as example of coupled devices with large bandwidth. The shape of the complete 3 dof system is represented in Fig. 4.

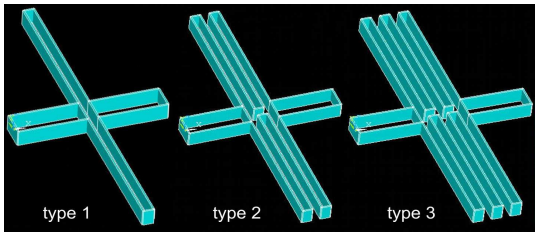

Fig. 3. Types of intermediate springs.

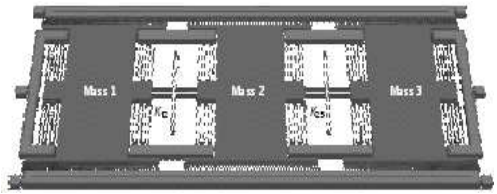

Fig. 4. Multi-dof harvester with amplified bandwidth.

Dynamic properties of a 3 dof energy harvester constituted by the same number of single devices are reported in Tab. 2 for some configurations. Figure 5a reports the modal displacement of the 3 dof harvester for modes I, II and III: the first mode is associated to the undeformed configuration (pure translation) of masses, the first resonance is consequently imposed by the stiffness of each separated harvester. Figure 5b represents the qualitative shape of the response function for the 3 dof harvester.

Tab. 2. FEM resonances of 3-dof harvesters

Design	Spring	Resonance frequency [Hz]		
		Mode I	Mode II	Mode III
B1	type 1	419	551	750
	type 2	419	485	598
	type 3	419	463	543
B7	type 1	356	508	723
	type 2	356	433	560
	type 3	356	408	499
B13	type 1	308	479	709
	type 2	308	397	536
	type 3	308	368	469

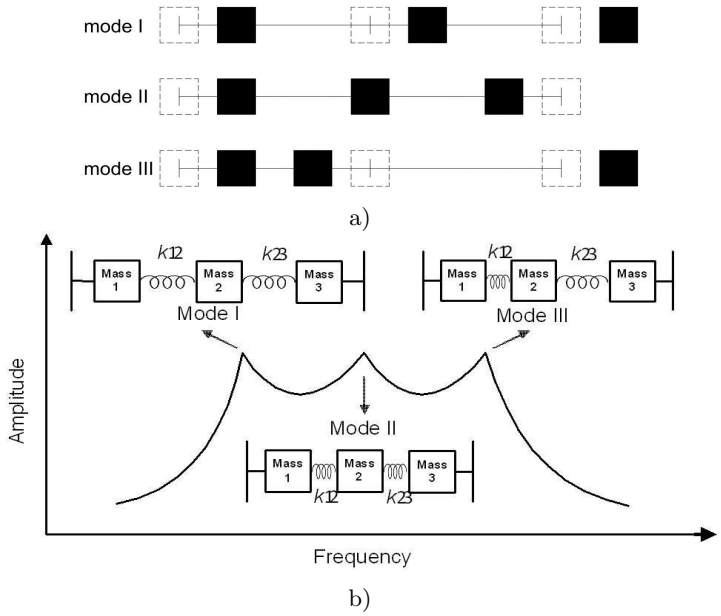

Fig. 5. Modal displacements of 3-dof harvesters (a) and qualitative frequency response function (b).

3.3. FEM models

Structural FEM models were built in order to simulate the static and dynamic behavior of harvesters; the commercial tool Ansys 11.0 was used. The vibrating part of the structure was modeled by using 10 nodes tetrahedral structural elements; a variable size was adopted for meshing the geometry in order to reduce the total amount of elements and the computation time. The elastic meander springs used to suspend the proof mass and the intermediate springs of multi-dof harvesters were simulated as well. Figure 6 reports an example of FEM model for the vibrating structure of the overlap harvester (design A) and for an intermediate spring. The spring stiffness was calculated by means of static analyses as the ratio between a unit force and the correspondent average displacement evaluated in four nodes. Modal simulations were performed to calculate the structural resonance frequency, to display the modal deformed shape associated to each resonance and to estimate the modal mass m_{mod}. Material properties assumed in the simulations for nickel were: Young's module $E = 195$ GPa, Poisson's ratio $\nu = 0.3$ and density $\rho = 8.9{\cdot}10^{-15}\mathrm{kg}/\mu\mathrm{m}^3$.

3.4. Electric set-up

The harvester device is based on the capacitive transduction principle; thus a static bias voltage is required to charge the armatures before the operations. The static voltage charge was provided by connecting the anchor to a voltage reference

v_0 and the suspended mass to the input voltage v_i (Fig. 7a). The same set-up must be provided for the preliminary characterization of the harvester, by using a common shaker as mechanical vibration source and a spectrum analyzer to monitor the power output (Fig. 7b).

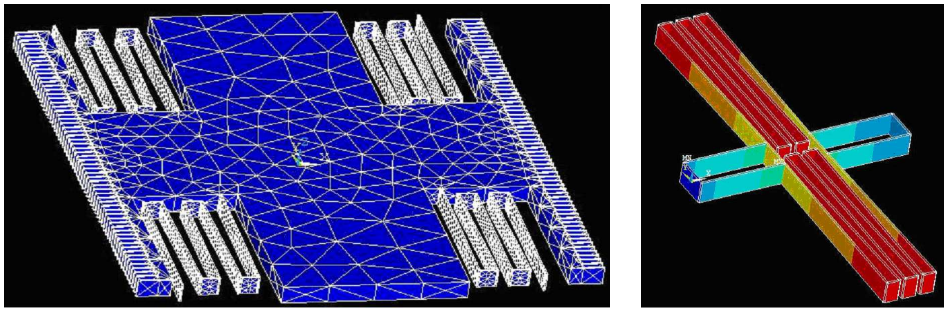

a) b)

Fig. 6. FEM model of the vibrating structure for design A (a) and qualitative FEM Von Mises stress distribution for an intermediate spring (b).

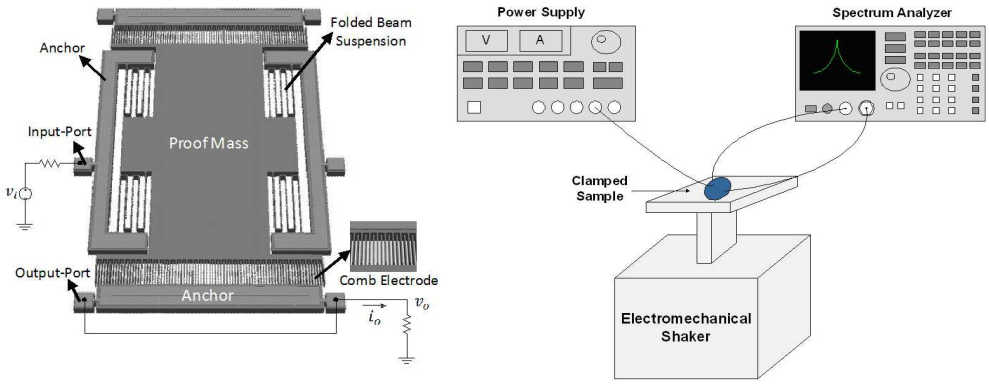

a) b)

Fig. 7. Electrical connections for the harvesting structure (a) and laboratory set-up for the preliminary performances characterization (b).

4. Fabrication process

The fundamental steps of fabrication process are reported in Fig. 8. The process started with a silicon wafer followed by a 2 μm silicon dioxide as electrical isolation layer between the silicon substrate and the eventual nickel harvester. Then, a 3 μm amorphous silicon layer (α-Si) was deposited by PECVD (Plasma Enhanced Chemical Vapor Deposition) to serve as a sacrificial layer (a). Next, patterned by the first mask using Shipley 1813 positive photoresist via lithography, via holes were dry etched through amorphous silicon to define the anchors (b). RIE (Reactive Ion

Etching) was used with the following conditions: 5 sccm and 45 sccm flow rate for O2 and SF6 respectively, 100 mT vacuum pressure, 100 W power, and 1.2 μm/min and 0.15 μm/min etch rate of amorphous silicon and photoresist respectively. Seeding layers (20 nm Cr and 25 nm Cu) were then evaporated (c) by means of an electro-beam evaporator for electroplating process. Then, electroplating mold in SU-8 photoresist (d) was patterned via UV lithography by using the second mask. SU-8 100 negative photoresist was adopted here because it allows generating ultra high features (which can be spun over 100 μm) with aspect ratios up to 20:1. The 100 μm thick nickel suspended microstructure (e) was then electroplated to create the body of the harvester. The release process allowed removing SU-8 and seed layers (f).

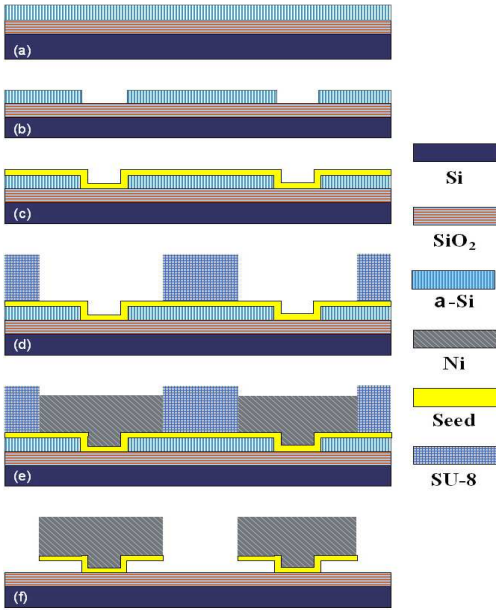

Fig. 8. Device cross section of fabrication process.

The electroplating process (Fig. 9) was conducted into an electrolyte solution at the temperature of 50°C; this temperature is low enough to allow the processing on pre-fabricated Integrated Circuits. The electroplating solution had a pH = 4 and consisted of nickel sulfamate (350 g/l), boric acid (40 g/l), nickel chloride (10 g/l) and sodium lauryl sulfate (1 g/l). The current density applied was about 10 mA/cm^2 and the electroplating speed was about 12 μm/hr. After electroplating, two different strategies were experienced for the releasing. Initially the NANOTM Remover PG was adopted to remove the SU-8 mold between 60°C to 80°C, followed by a plasma etching process to remove the SU-8 residues and by the application of chromium and cupper etchants to remove the seed layers. Finally, a unique dry etching process was adopted to remove amorphous silicon sacrificial layer. The second releasing strategy was preferable because it is able to minimize the possibility of stiction among counterparts, especially for the relatively huge proof mass adopted in the design. Compared

to the wet releasing process which introduces some inherent problems like stiction and low etch rate, dry releasing process provides good efficiency on etch rate, Si to SiO_2 selectivity and can be compatible with post-CMOS integration processes. Figure 10 shows some details of the harvester after building process and the complete device (design B) from Scanning Electron Microscope (SEM).

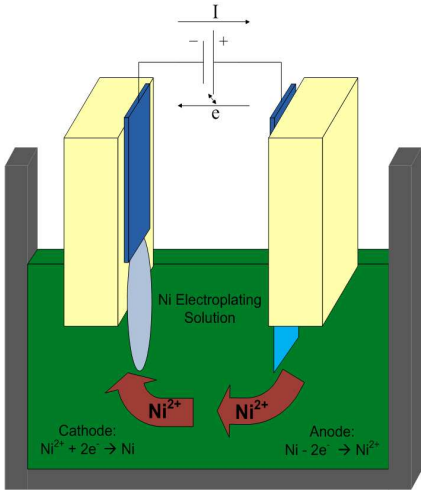

Fig. 9. Schematic for nickel electroplating process.

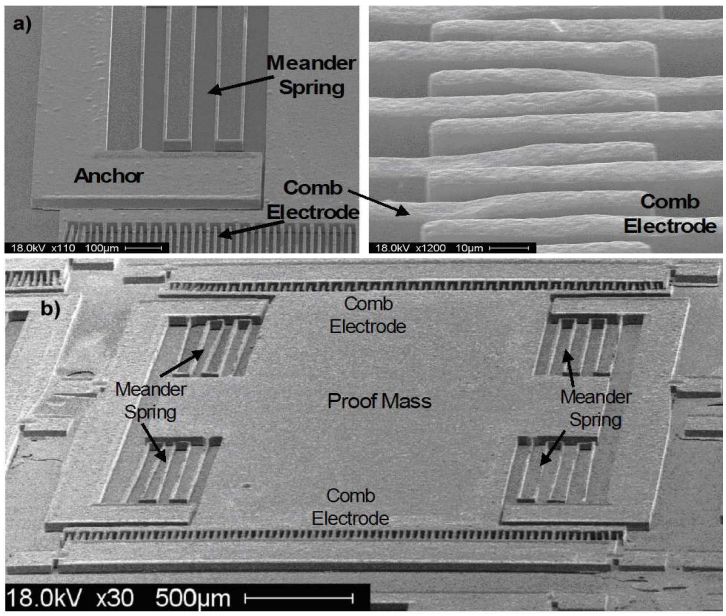

Fig. 10. SEM pictures of energy harvester after fabrication process: details of anchor, meander spring and comb electrodes (a) and design B complete device (b).

5. Voltage rectification

In order to supply the sensors or to charge a battery, the voltage output generated by the harvester must be rectified. This rectification can be operated by means of a simple configuration of electronic components. Two solutions are possible: single diode or multiple diodes (diodes bridge) associated to a leveling capacitor. Both solutions are represented in Fig. 11, where the harvester is indicated as H, the leveling capacitor as C_L, and the diodes as D_i. A voltage reference (VR) is also added in parallel to the leveling capacitor.

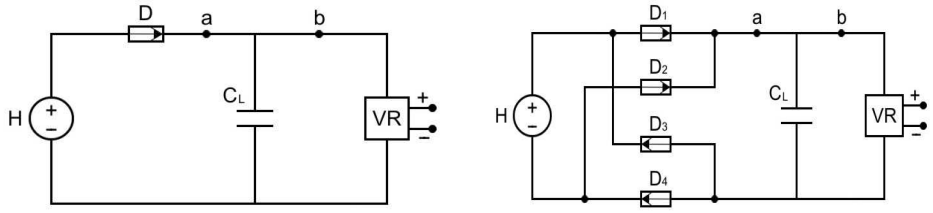

a) b)

Fig. 11. Rectification of the harvested voltage by single (a) and multiple (b) diodes solutions.

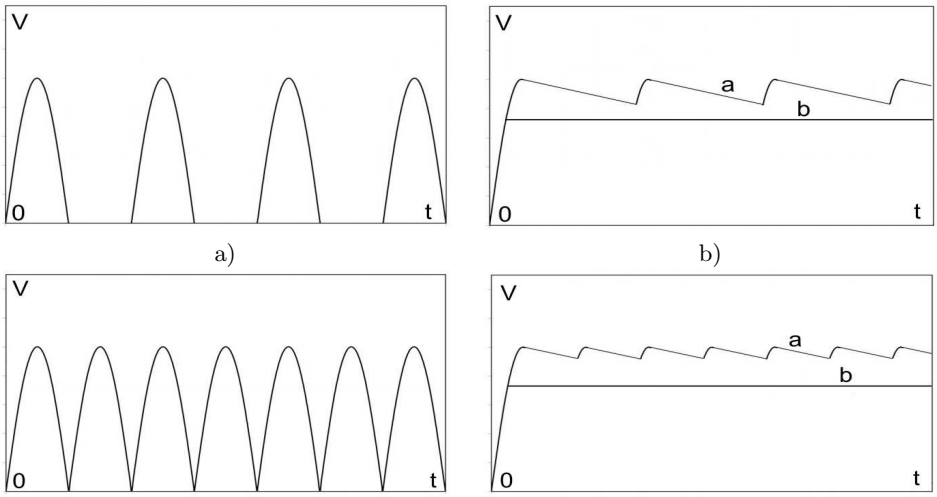

a) b)

c) d)

Fig. 12. Voltage curve in the time domain. Single (a, b) and multiple (c, d) diodes solution.

If a sinus voltage is assumed as output for the harvester, the portion of the curve corresponding to negative voltages is cut by the single diode (Fig. 12a). Figure 12b represents the voltage variation in the circuit after the capacitor (curve a) and after the voltage reference device (curve b) respectively. The described solution is suitable for that environments associated to high vibrating energy levels because the efficiency

of the energetic conversion is quite low. This is due to the loss of a relevant portion of the original alternate voltage curve. The slope of segments reported in Fig. 12b (curve a) is proportional to the capacitance of the leveling capacitor (C_L) and to the sensing system energetic requirements.

To increase the efficiency of the energetic conversion, the diodes bridge configuration is needed. The bridge is represented by four diodes connected as reported in Fig. 11b. The presence of multiple diodes allows increasing the number of voltage peaks on the positive region of the diagram, as visualized by Fig. 12c. The voltage variation in the circuit after the capacitor and after the voltage reference device is represented in Fig. 12d (curve a and b respectively). The multiple diode solution allows reducing the time interval between two successive charges of the leveling capacitor C_L; this improves the average level of its charge under the same excitation conditions.

6. Modular approach for integrated self-powered sensing systems

Many vehicular applications involve inertial sensors such as one-dimensional or multi-dimensional accelerometers, gyroscopes, inclinometers, etc. Inertial sensors fabricated by MEMS technology are generally based on the same working principle as MEMS harvesters presented before, i.e. the capacitive transduction. Despite the structural shape of multiaxial sensors is more complicated than the single axis configuration, they are composed by the same basic elements: proof mass (usually represented by a suspended plate), supporting springs and comb drives. It descends that the same fundamental structural elements are present in harvesters and inertial sensors designs, making their structures comparable and leading to the possibility of a common and simultaneous fabrication process. The use of a single building process for harvesters and inertial sensors allows designing these devices on a single substrate in order to obtain a compact self-powered system. The main advantages of this approach are: (a) to reduce the dimensions, (b) to reduce the energy losses due to dissipations, (c) to allow the system customization according to the vibrating conditions, (d) to simplify the building process, (e) to reduce the building costs, and (f) to avoid misalignments between the axis of adjacent sensors.

The coexistence of sensors and harvesters on the same substrate needs to define a specific procedure for the layout definition. Firstly the number and typology of sensors must be decided according to the application; the total amount of sensors for device is limited by their energetic requirements and by the power associated to the vibrations. In a successive phase, the number of harvesters needed to provide the desired amount of energy must be calculated. The presence of multiple harvesters increases the global efficiency in environments with variable vibration frequencies; this is possible by adopting a series of several harvesters with a resonance frequency lightly different, that allows one or two harvesters always to resonate. The result is a significant amplification of the global bandwidth of the system. The harvester resonance frequency is a function of its structural dimensions and material properties;

the desired resonance can be simply obtained by a proper dimensioning of a few elements such as the supporting beams or the central plate. Compact equations for the evaluation of the resonance frequency of suspended structures were proposed in [35].

Microfabrication process adopted to build MEMS structures usually requires one or more masks for the photolithography steps; this is a crucial phase for self-powered systems design and must be carefully considered. The final mask might be quite complicated according to the number of structures included, considering both sensors and scavengers. It is necessary to define a schematic approach to create the mask with a small number of simple operations. The best solution to easily design the mask is a modular approach with the repetition of single modules previously defined. Each module contains a movable structure and the electrical connections. The number and the typology of structures must be defined in advance and each module must contain all specific details about the structural dimensions. The structure defined by each module may be used as sensor or as energy harvester according to the function previously assigned to it. Only few modules are sufficient to define the mask of self-powered systems containing a single harvester and a single sensor. A possible collection of the basic modules is represented in Fig. 13. The suspended structure is represented qualitatively as a standard icon; the real structure needs to be defined in advance according to structural dimensioning results, as well as the internal electric connections with the electrodes. The module of a single harvester (Fig. 13a), of a single one-axis sensor (Fig. 13b), two-axis sensor (Fig. 13c) and three-axis sensor (Fig. 13d) are reported respectively. The modules defining the harvester present a couple of output terminals; the modules defining the sensors present a couple of input terminals and a series of output terminals, the number of which is proportional to the number of their sensing axis (plus one terminal for the output voltage reference).

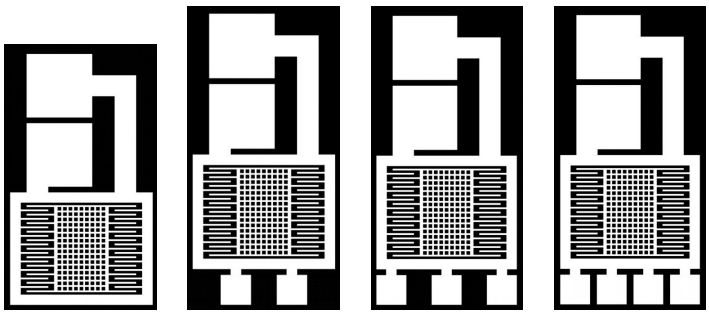

Fig. 13. Basic modules for the mask definition of single harvesters (a), one-axis (b), two-axis (c) and three-axis (d) inertial sensors.

Self-powered systems composed by multiple harvesters and/or sensors can be defined as well; their mask must be created with the combination of several modules. The total number of different modules is limited but their assembling allows defining complicated masks for extended self-powered sensing systems. The fundamental mod-

ules for multiple structures configurations are depicted in Fig. 14, where three-axis sensors are considered.

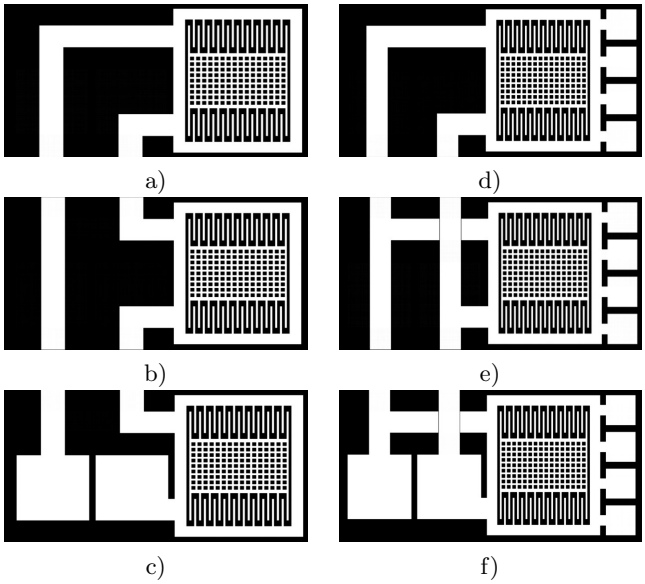

Fig. 14. Modules for the mask definition of systems with multiple harvesters (a–c) and/or triple-axis inertial sensors (d–f).

The combination of several modules for harvesters and sensors allows creating complicated masks; an example of a complete mask is reported in Fig. 15 where a self-power system having 10 harvesters and 3 triple-axis inertial sensors is represented. The resulting system can be packaged and wire bonded in correspondence to the contact pads which define the harvesters output (on the left), the sensors inputs (on the bottom) and the sensors outputs (on the right). A connection with the proper conditioning circuit must be provided according to the specific application [36].

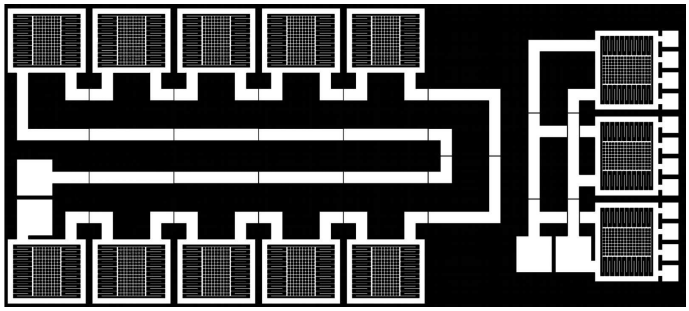

Fig. 15. Example of a complete mask for a self-powered sensing system.

7. Conclusions

MEMS-based vibration energy harvesters for low frequency self-powered vehicular sensing systems were designed and built by using nickel electroplating technique. Several design variants were introduced and a strategy for bandwidth amplification was adopted and fully explored in order to increase the efficiency of the device. Finite element (FEM) simulations were conducted to verify the design methodologies presented. A modular approach was introduced for the fabrication and mask definition of integrated self-powered sensing platforms. Initial results hold great promise for improving the efficiency of the energy harvesters.

Acknowledgments. The authors thank Prof. A. Somà and Dr. J. Wang for the support given to the work, and the NNRC (Nanomaterials and Nanomanufacturing Research Center) at USF of Tampa (Florida, USA) for the facilities provided.

References

[1] POHL A., SEIFERT F., *Wirelessly interrogable SAW-sensors for vehicular applications*, *Proc. IEEE Instrumentation and Measurement Technology Conference*, Brussels, Belgium, pp. 1465–1468, 1996.

[2] PELCZAR C., SUNG K., KIM J., JANG B., *Vehicle speed measurement using wireless sensor nodes*, *Proc. IEEE International Conference on Vehicular Electronics and Safety*, Columbus, OH, USA, pp. 195–198, 2008.

[3] PARADISO J., STARNER T., *Energy scavenging for mobile and wireless electronics*, Pervasive Computing, pp. 18–27, 2005.

[4] SHEA H.R., *Reliability of MEMS for space applications*, Proc. of SPIE Reliability, Packaging, Testing and Characterization of MEMS/MOEMS, **6111**, 2006.

[5] BRUNELLI D., BENINI L., MOSER C., THIELE L., *An efficient solar energy harvester for wireless sensor nodes*, Proc. Design, Automation and Test in Europe (DATE), Dresden, Germany, pp. 104–109, 2008.

[6] TANG W.C., NGUYEN T.H., HOWE R.T., *Laterally driven polysilicon resonant microstructures*, Sensors and Actuators A-Physics, vol. **20**, pp. 25–32, 1989.

[7] FLYNN A.M., SANDERS S.R., *Fundamental limits on energy transfer and circuit considerations for piezoelectric transformers*, IEEE Transactions on Power Electronics, vol. **17** (1), pp. 8–14, 2002.

[8] WILLIAMS C.B., SHEARWOOD C., HARRADINE M.A., MELLOR P.H., BIRCH T.S., YATES R.B., *Development of an electromagnetic micro-generator*, Proc. of IEE Circuits, Devices et Systems, vol. **148** (6), pp. 337–342, 2001.

[9] BEEBY S.P., TUDOR M.J., WHITE N.M., *Energy harvesting vibration sources for microsystems applications*, Measurements Science and Technology, vol. **17**, pp. 175–195, 2006.

[10] MITCHESON D., YEATMAN M., KONDALA RAO G., HOLMES S., GREEN T.C., *Energy harvesting from human and machine motion for wireless electron devices*, Proc. of the IEEE, vol. **96** (9), pp. 1457–1486, 2008.

[11] ROUNDY S., *Energy scavenging for wireless sensor networks with special focus on vibrations*, Kluwer Academic Publishers, 2003.

[12] R. XIA, C. WONJAE CHOI, S.G. KIM, *Self-powered wireless sensor system using MEMS piezoelectric micro power generator*, Proc. of 5th IEEE Conference on Sensors, Daegu, Korea, pp. 6–9, 2006.

[13] JEN B.C., LANG J.H., *A variable-capacitance vibration-to-electric energy harvester*, IEEE Transactions on Circuits and Systems I, **53**(2), pp. 288–295, 2006.

[14] RAGHUNATHAN V., CHOU P.H., *Design and power management of energy harvesting embedded systems*, Proc. of International Symposium on Low Power Electronics and Design (ISLEPED), Tegernsee, Germany, pp. 369–374, 2006.

[15] ROUNDY S., LELAND E.S., BAKER J., CARLETON E., REILLY E., LAI E., OTIS B., RABAEY J.M., WRIGHT P.K., SUNDARARAJAN V., *Improving power output for vibration-based energy scavengers*, IEEE Pervasive Computing, vol. **4**, pp. 28–36, 2005.

[16] SOMÀ A., DE PASQUALE G., BRUSA E., BALLESTRA A., *Effect of residual stress on the mechanical behaviour of microswitches at pull-in*, Strain, in press.

[17] PEANO F., TAMBOSSO T., *Design and optimization of a MEMS electret-based capacitive energy scavenger*, Journal of Microelectromechanical Systems, vol. **14** (3), pp. 429–435, 2005.

[18] PEANO F., COPPA G., SERAZIO C., PEINETTI F., D'ANGOLA A., *Nonlinear oscillations in a MEMS energy scavenger*, Mathematical and Computer Modelling, vol. **43**, pp. 1412–1423, 2006.

[19] DE PASQUALE G., VEIJOLA T., *Comparative numerical study of FEM methods solving gas damping in perforated MEMS devices*, Microfluidics and Nanofluidics, vol. **5** (4), pp. 517–528, 2008.

[20] DE PASQUALE G., VEIJOLA T., SOMÀ A., *Modelling and validation of air damping in perforated gold and silicon MEMS plates*, Journal of Micromechanics and Microengineering, in press.

[21] MUHLSTEIN C.L., STACH E.A., RITCHIE R.O., *Mechanism of fatigue in micron-scale films of polycrystalline silicon for microelectromechanical systems*, Applied Physical Letters, vol. **80** (9), pp. 1532–1534, 2002.

[22] BHALERAO K., SOBOYEJO A.B., SOBOYEJO W.O., *Modeling of fatigue in polysilicon MEMS structures*, Journal of Materials Science, vol. **38** (20), pp. 4157–4161, 2003.

[23] SHARPE W.N., BAGDAHN J., JACKSON K., COLES G., *Tensile testing of MEMS materials – recent progress*, Journal of Materials Science, vol. **38** (20), pp. 4075–4079, 2003.

[24] DE PASQUALE G., SOMÀ A., *Reliability in MEMS: design of gold devices for mechanical fatigue tests*, Romanian Journal of Information Science and Technology, vol. **11** (2), pp. 177–191, 2008.

[25] DE PASQUALE G., SOMÀ A., *MEMS mechanical fatigue: experimental results on gold microbeams*, Journal of Microelectromechanical Systems, vol. **18** (4), pp. 828–835, 2009.

[26] DE PASQUALE G., BRUSA E., SOMÀ A., *Capacitive vibration harvesting with resonance tuning*, Proc. of Symposium on Design, Test, Integration and Packaging of MEMS/MOEMS (DTIP), Rome, Italy, pp. 280–285, 2009.

[27] CHALLA V.R., PRASAD M.G., SHI Y., FISHER F.T., *A vibration energy harvesting device with bidirectional resonance frequency tunability*, Smart Materials and Structures, vol. **17**, 015035, 2008.

[28] SHAHRUZ S.M., *Design of mechanical band-pass filters for energy scavenging*, Journal of Sound and Vibrations, vol. **292**, pp. 987–998, 2006.

[29] GENTA G., *Vibration of structures and machines*, New York: Springer Verlag, 1999.

[30] CORNWELL P.J., GOETHAL J., KOWKO J., DAMIANAKIS M., *Enhancing Power Harvesting using a Tuned Auxiliary Structure*, Journal of Intelligent Material Systems and Structures, vol. **16**, pp. 825–834, 2005.

[31] LELAND E.S., WRIGHT P.K., *Resonance tuning of piezoelectric vibration energy scavenging generators using compressive axial preload*, Smart Materials and Structures, vol. **15**, pp. 1413–1420, 2006.

[32] DE PASQUALE G., SIYAMBALAPITIYA C., SOMÀ A., WANG J., *Performances improvement of MEMS sensors and energy scavengers by diamagnetic levitation*, Proc. of International Conference on Electromagnetics in Advanced Applications (ICEAA), Torino, Italy, pp. 465–468, 2009.

[33] DE PASQUALE G., SOMÀ A., *Investigations on energy scavenging methods using MEMS devices*, Proc. International Semiconductor Conference (CAS), Sinaia, Romania, vol. **1**, pp. 163–166, 2008.

[34] DE PASQUALE G., WEI M., SOMÀ A., WANG J., *Capacitive MEMS energy harvesters for structural monitoring: design and fabrication*, Proc. International Semiconductor Conference (CAS), Sinaia, Romania, vol. **1**, pp. 211–214, 2009.

[35] DE PASQUALE G., SOMÀ A., *Numerical and experimental validation of out-of-plane resonance closed formulas for MEMS suspended plates with square holes*, Microsystem Technologies, vol. **15** (3), pp. 391–400, 2009.

[36] DE PASQUALE G., SOMÀ A., *Wireless system for measurement and transmission of dynamic excitations, railway bogie including this system and dedicated control methods*, Italian Patent, application number: TO2009A000247, March 31st, 2009.